J Mater Sci (2007) 42:1694–1708
DOI 10.1007/s10853-006-0968-9

Review on the fracture processes in nanocrystalline materials

I. A. Ovid'ko

Received: 30 May 2006 / Accepted: 12 September 2006 / Published online: 9 January 2007

Abstract An overview of experimental study, computer simulations and theoretical models of fracture of nanocrystalline materials is presented. The key experimentally detected facts on ductile and brittle fracture processes are discussed. Special attention is paid to computer simulations and theoretical models of nucleation and growth of nanocracks and nanopores in deformed nanocrystalline materials. Also, we discuss mechanisms for fracture suppression in such materials showing good ductility or superplasticity.

Introduction

Nanocrystalline materials—polycrystals with grain sizes less than 100 nm—have the unique mechanical properties highly desirable for a wide range of applications; see, e.g., [1–12]. For instance, they often exhibit extremely high strength, superhardness and good fatigue resistance [1–12]. At the same time, in most cases, these materials show low tensile ductility at room temperature, which essentially limits their practical utility. However, recently several examples of substantial tensile ductility and even superplasticity of nanocrystalline materials have been reported [13–31]. With these experimental data, of particular interest are the generic structural features and phenomena responsible for unique combination of high strength and good ductility of these materials. In particular, in order to understand the fundamentals of the outstanding mechanical properties of nanocrystalline materials, it is very important to experimentally characterize and theoretically describe fracture mechanisms operating in these systems. The main aim of this paper is to review experimental research, computer simulations and theoretical models of fracture of nanocrystalline materials. Also, special attention is paid to the origin of fracture suppression in nanomaterials showing good ductility or superplasticity.

I. A. Ovid'ko (✉)
Institute of Problems of Mechanical Engineering,
Russian Academy of Sciences, Bolshoj 61, Vas.Ostrov,
St. Petersburg 199178, Russia
e-mail: ovidko@def.ipme.ru

Ductile and brittle fracture modes in nanocrystalline materials: general aspects

The fracture behavior of nanocrystalline materials is not well defined because of many factors influencing deformation and fracture processes. Nevertheless, with available experimental data in this area, one can distinguish several tendencies in the fracture behavior of such materials. First of all, both ductile and brittle fracture processes occur in nanocrystalline materials. There are several examples of materials having an average grain size in the range from 20 to 100 nm and showing ductile fracture with preceding neck formation and dimpled structures at fracture surfaces [4, 23, 28–33]. In doing so, ductile fracture is viewed to occur through the microvoid coalescence mechanism. A typical dimpled structure is illustrated in Fig. 1 showing scanning electron microscopy image of the facture surface of a bulk nanocrystalline Al-5%Mg alloy after tensile testing to failure. Artifact-free Al-5%Mg alloy bulk specimens with an average grain size of around

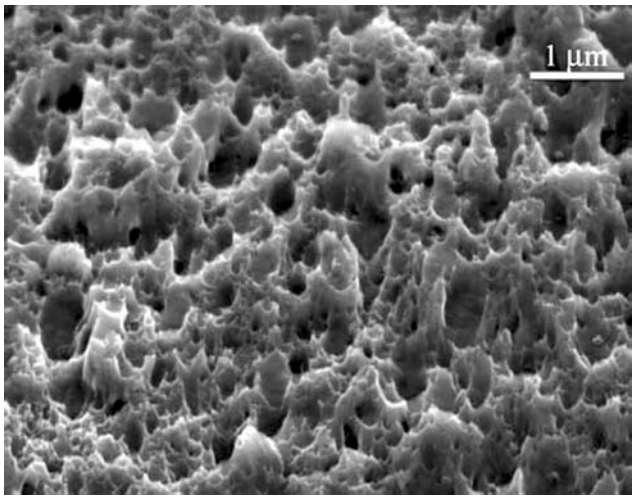

Fig. 1 Dimpled structures at the fracture surface of the nanocrystalline Al–5%Mg alloy after tensile testing to failure [Reprinted from [32], copyright (2006), with permission from Elsevier]

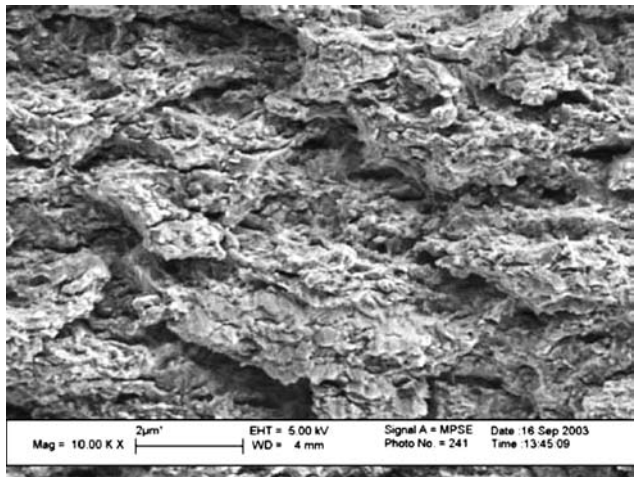

Fig. 2 Fracture surface morphology of a nanocrystalline Ni specimen cyclically loaded to failure at a maximum stress of 850 MPa (with fatigue load ratio = 0.25) and a frequency of 0.2 Hz at room temperature in air [Reprinted from [35], copyright (2006), with permission from Elsevier]

26 nm and a relatively narrow grain size distribution were synthesized by an in situ consolidation mechanical alloying technique [31]. These samples demonstrated ultrahigh strength (for instance, ultimate tensile strength is around 740 MPa), good tensile ductility (8.5% elongation) and ductile fracture behavior with the dimpled features at the fracture surface (Fig. 1).

At the same time, nanocrystalline Ni-15%Fe specimens with an average grain size of around 9 nm [32, 32] and fatigued nanocrystalline Ni specimens with an average grain size of around 30 nm [34] exhibit intergranular brittle fracture. Also, brittle fracture with dominant intergranular cracking occurs in superhard nanoceramic coatings [3]. In these cases, the main brittle crack is treated to be formed by the generation of multiple intergranular nano/micro-scale cracks and their convergence. The intergranular brittle fracture mode is illustrated by Fig. 2 showing scanning electron microscopy image of the facture surface of a nanocrystalline Ni specimen cyclically loaded to failure. Nanocrystalline Ni specimens with an average grain size of around 30 nm were fabricated by electrodeposition and subjected to low cycle fatigue load [34]. These samples demonstrated cyclic strain hardening and brittle behavior. In particular, fracture surface examination revealed a load-frequency-independent brittle fracture morphology (Fig. 2), in contrast to the more ductile dimpled morphology found for monotonic loading conditions in similar specimens [34]. This example is indicative of the sensitivity of the fracture mode in nanocrystalline Ni to conditions of load.

In general, fracture processes in nanocrystalline materials are crucially influenced by the large amount of grain boundaries. Such boundaries serve as preferable places for nanocrack nucleation and growth, because the atomic density is low, and interatomic bonds are weak at grain boundaries compared to the bulk phase. In the case of ductile fracture carried by microvoid coalescence, grain boundaries with their high diffusivity enhance the microvoid growth, a process mediated by diffusion. Besides, the extra energy of grain boundaries contributes to the driving force for intergranular fracture with cracks propagating along boundaries and releasing the extra energy, compared to intragranular fracture with cracks propagating through grain interiors. At the same time, grain boundaries are short and curved at numerous triple junctions in nanocrystalline materials. Therefore, if cracks tend to nucleate and grow along grain boundaries, geometry of grain boundary ensembles causes restrictions on intergranular fracture processes.

With the large amount of grain boundaries in nanocrystalline materials, there is a strong competition between intergranular and intragranular fracture processes. Either one of these processes dominates or they occur in concurrent way in materials, depending on their material and structure parameters as well as on the conditions of loading. Besides, fracture processes in nanocrystalline materials compete and interact with plastic deformation processes that have the unique peculiarities due to both the nanoscale and interface effects. In particular, with nanoscale sizes of grains and the large amount of grain boundaries, plastic

deformation in nanocrystalline materials is characterized by very high values of the flow stress. Plastic deformation in such materials effectively occurs by lattice dislocation slip and deformation mechanisms mediated by grain boundaries [1–12]. The lattice dislocation slip is dominant in materials with intermediate grains having the size d in the range from d_c to 100 nm, where the critical grain size d_c (=10–30 nm) depends on material and structure parameters. Basic carriers of the lattice dislocation slip in intermediate grains are perfect and partial dislocations emitted from grain boundaries; see, e.g., [35–38]. Deformation mechanisms mediated by grain boundaries are dominant in materials with finest grains having the grain size $d < d_c$. These mechanisms are grain boundary sliding, grain boundary diffusional creep (Coble creep), triple junction diffusional creep and rotational deformation mode; see, e.g., [1–12]. In the context discussed, one expects that fracture processes in a nanocrystalline material are sensitive to the grain size because of its dramatic effect on plastic deformation mode operating and competing with fracture in the material.

Li and Ebrahimi [32, 33] reported that reduction in grain size causes a shift in fracture mode, from ductile mode (for nanocrystalline Ni with mean grain size around 44 nm) to brittle fracture (for nanocrystalline Ni-15%Fe alloy with mean grain size around 9 nm). However, the discussed experiments dealt with the materials—pure Ni and Ni-15%Fe alloy—having different chemical compositions. Therefore, the shift in fracture mode [32, 33] is influenced by both the grain size and chemical composition effects. In these circumstances, the grain size effect cannot be unambigiously identified. Nevertheless, the grain refinement commonly leads to increase in the flow stress. In this case, with reduction in grain size, values of the flow stress become closer to those needed to induce fast fracture processes, and fracture mode tends to shift from slow ductile mode to fast brittle fracture. It is just a tendency (but not a rule) that needs further investigation.

The effect of an average grain size on fracture mode can manifest itself through its effects on plastic flow and diffusivity in nanocrystalline materials. Accelerated diffusion along grain boundaries and intensive plastic flow (by lattice dislocation slip and/or deformation mechanisms mediated by grain boundaries) provide effective relaxation of local stress inhomogeneities and thereby suppress the brittle behavior. With the existence of a critical grain size d_c for transition from the lattice dislocation slip to deformation mechanisms mediated by grain boundaries, it would be interesting to check, if the size d_c plays a role in transition in fracture mode in nanocrystalline materials. In this context, of particular interest are the experiments [28–31] which are indicative of ductile fracture in nanocrystalline pure Cu and Al-5%Mg alloy with average grain sizes being 23 and 26 nm, respectively. The grain size values in these materials are very small and close to the critical size (d_c = 10–30 nm) for transition from the lattice dislocation slip to deformation mechanisms mediated by grain boundaries. However, the microstructural characterization [29] of nanocrystalline Cu samples unambigiously shows the lattice dislocation slip to be active. In this situation, with a very high level of the applied stress, void growth by lattice dislocation emission can effectively occur [39] and contribute to ductile fracture processes.

Besides grain size, other factors strongly affect fracture in nanocrystalline materials. In particular, crack nucleation and propagation can be dramatically enhanced due to fabrication-produced pores and contaminations. This effect of artifacts has been demonstrated in the experiments [40] dealing with fracture of nanocrystalline Ni films fabricated by DC magnetron sputtering and pulsed laser deposition. Following [40], the nanocrystalline Ni film material fabricated by DC magnetron sputtering and characterized by a narrow distribution in grain size (with an average grain size of around 19 nm) contains pores and behaves in a brittle manner, with failure occurring via rapid coalescence of intergranular cracks. At the same time, the nanocrystalline Ni film material fabricated by pulsed laser deposition and characterized by a narrow distribution in grain size (with an average grain size of around 17 nm) is free from pores and behaves in a ductile manner, with failure occurring via slow ductile crack growth [40].

Nucleation of nanocracks at grain boundaries and their triple junctions

To understand the specific fracture behavior of the nanocrystalline matter, results of microstructural experimental characterization of nanocrystalline materials under mechanical load are of crucial importance. Following experimental data [23], nanovoids in ductile nanocrystalline Ni commonly nucleate and grow at grain boundaries and their triple junctions during tensile deformation (Fig. 3). In these experiments, nanocrystalline Ni specimens (with an average grain size of around 30–40 nm and a narrow grain size distribution) fabricated by electrodeposition were subjected to tensile tests performed ''in situ'' in the transmission electron microscope (TEM). Damage

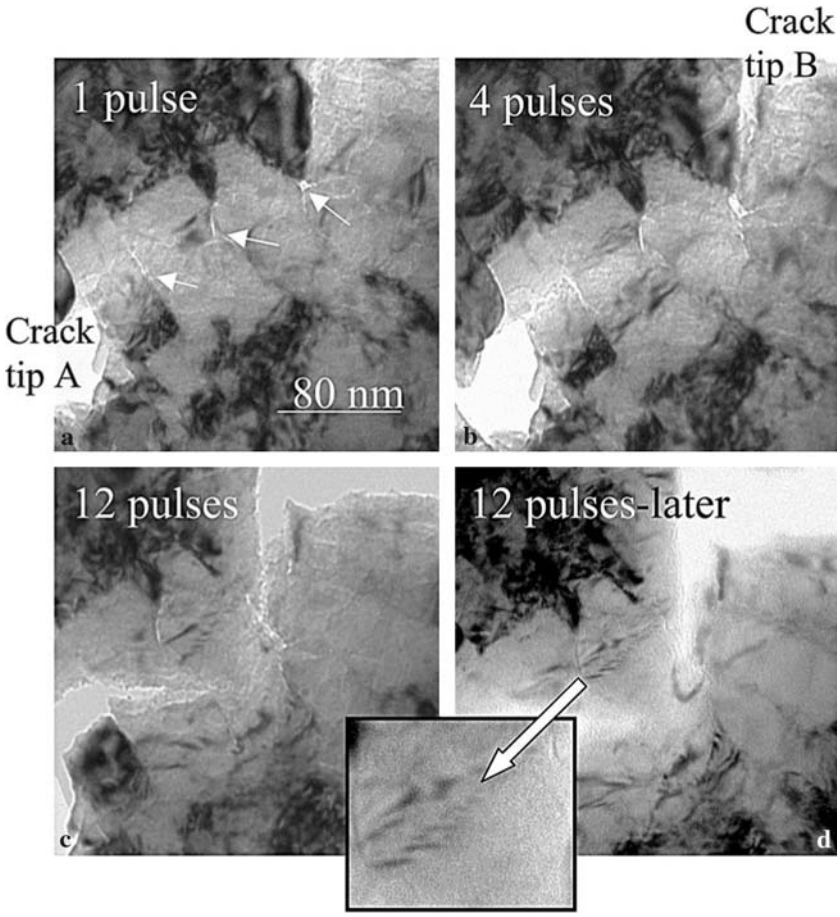

Fig. 3 A sequence of ''freeze-frame'' images captured during an in situ deformation test in the transmission electron microscope of a nanocrystalline Ni specimen. Images (**a**–**d**) show the microstructural evolution and progression of damage with an increase in the plastic strain induced by applied displacement pulses. The presence of grain boundary cracks and triple-junction voids (indicated by *white arrows* in **a**), and their growth in (**b**–**d**) are shown. The magnified inset in (**d**) highlights the dislocation activity [Reprinted from [23], copyright (2003), with permission from Elsevier]

evolution at the nanoscale level in these specimens is presented in Fig. 3 showing a sequence of ''in situ'' TEM images of the microstructure of a nanocrystalline Ni specimen during plastic deformation. As follows from the images (Fig. 3), grain boundaries and their triple junctions serve as preferred places for nucleation of nanoscale voids in vicinity of a large crack. The large crack grows along grain boundaries and absorbs the nanovoids (Fig. 3).

A similar view on fracture processes at the nanoscale level is given by molecular dynamics simulations [42–44]. These simulations show that nanocracks tend to be generated at triple junctions of grain boundaries near tips of pre-existent large cracks in nanocrystalline Ni and nanocrystalline α-Fe with grain size ranging from 5 to 12 nm and from 6 to 12 nm, respectively. In the context discussed, with a very high volume fraction of triple junctions of grain boundaries in nanocrystalline materials, nanocracks at triple junctions can be treated as typical elemental carriers of fracture in such materials. This causes particular interest in understanding the mechanisms for nanocrack generation at triple junctions and their correlation with plastic deformation processes mediated by grain boundaries. In paper [44], a theoretical model has been suggested describing nucleation and growth of nanocracks at triple junctions due to grain boundary sliding. Below we will consider in detail the basic statements of the model [44], because it is concerned with typical nanocracks and relates the specific nanostructural features with fracture mechanisms operating in mechanically loaded nanocrystalline materials.

The model [44] describes fracture processes in nanocrystalline materials in which grain boundary sliding essentially contributes to plastic flow. Grain boundary sliding commonly occurs by either local shear events [45–47] or movement of grain boundary dislocations [46–49] and leads to accumulation of sessile dislocations at triple junctions [47, 48]. In the case of dislocation mode of grain boundary sliding, mobile grain boundary dislocations (with the Burgers vectors parallel to grain boundary planes) move causing the sliding in a mechanically loaded specimen (Fig. 4a). They are stopped at triple junctions of grain boundaries, where boundary planes are curved and thereby dislocation movement is hampered (Fig. 4a).

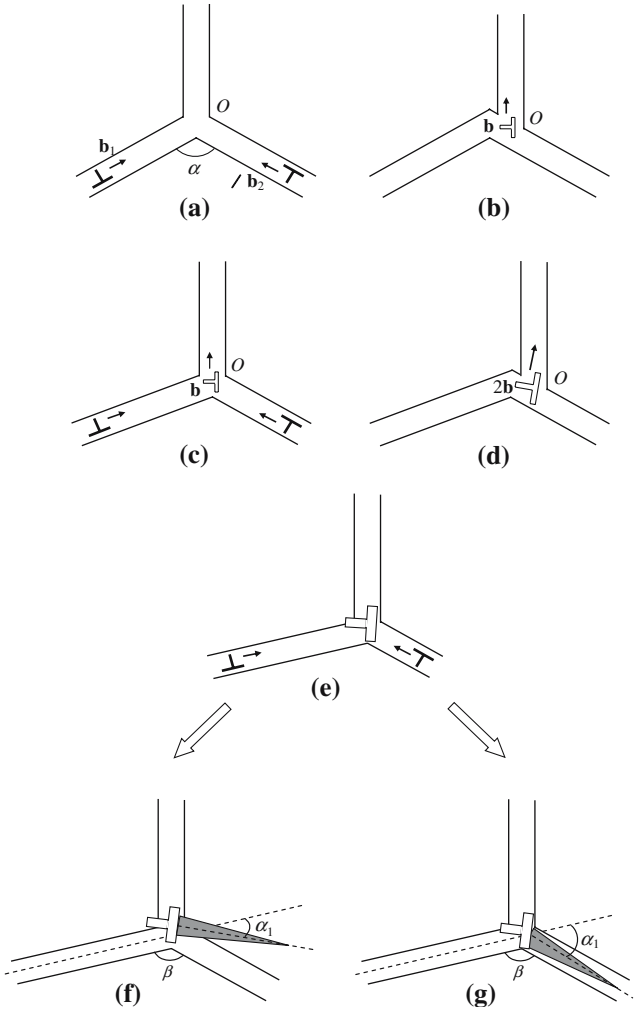

Fig. 4 Grain boundary sliding causes formation of triple junction dislocation (**a**)–(**e**) whose stress field induces generation of nanocrack either in grain interior (**f**) or along a grain boundary (**g**). The angle β between grain boundary planes and the angle α_1 between the nanocrack plane and one of grain boundary planes are shown (**f**) and (**g**)

Further movement of grain boundary dislocations needs an increase of the applied stress. When the applied stress increases, grain boundary dislocations reach a triple junction and come into dislocation reaction resulting in the formation of a sessile dislocations at the junction (Fig. 4b) [47, 48]. This process is an elementary act of (super)plastic deformation involving grain boundary sliding in nanocrystalline materials where amount of triple junctions is large. The process repeatedly occurs in a deformed nanocrystalline specimen and gives rise to an increase of the Burgers vector of the sessile dislocation (Fig. 4c–e). (Also, accumulation of the sessile dislocations at triple junctions occurs in a similar way in the situation where grain boundary sliding is carried by local shear events [47].) Following [44], a nanocrack at the triple junction is generated to release the strain energy of the sessile dislocation when its Burgers vector magnitude achieves a critical value (Fig. 4f, g). In doing so, the nanocrack may nucleate either in the grain interior (Fig. 4f) or along a grain boundary adjacent to the triple junction (Fig. 4g).

In general, the energetically favorable generation of a crack/nanocrack is characterized in the first approximation by its equilibrium length L_e; see, e.g., [44, 50, 51]. The equilibrium length L_e of a nanocrack is defined as the nanocrack length corresponding to the maximum or minimum energy of the system. In the first case, a nanocrack tends to rapidly grow (shrink), if its length L is larger (lower, respectively) than the equilibrium length L_e. That is, the equilibrium state of the nanocrack with the length $L = L_e$ is unstable. In the second case (the system energy has a minimum at $L = L_e$), the generation and growth of a nanocrack with the length $L < L_e$ are energetically favorable until its length L reaches L_e. That is, the equilibrium state of the nanocrack with the length $L = L_e$ is stable. This case includes, in particular, the generation and growth of a triple junction nanocrack (Fig. 4f, g). These processes are energetically favorable, if the nanocrack length L is lower than the equilibrium length L_e. The equilibrium state of the triple junction nanocrack with the length $L = L_e$ is stable, because the dislocation stress field rapidly falls with increasing distance from the dislocation line, while the external stress weakly influences the nanocrack generation [44].

In calculation of L_e, Ovid'ko and Sheinerman [44] used the configurational force method [50] that was effectively exploited in analysis of the generation of plane microcracks in the stress fields of superdislocations [50], dislocation pile-ups [50], disclination loops [52] and wedge line disclinations [51]. The method [50] was developed for a description of conditions for the energetically favored generation/growth of cracks in the local stress fields of internal defects—first of all, dislocations—formed due to inhomogeneous plastic flow in solids. This approach and the classical Griffith' theory (describing the external-stress-induced growth of cracks) are treated to be complementary. Indenbom [50] considered solids with dislocations creating stress fields whose relaxation occurs by the generation of cracks. In the framework of the approach [50], a flat crack in a solid is described as an ensemble of continuously distributed virtual dislocations. In these circumstances, the crack generation is equivalent to the generation of the virtual dislocations, and the criterion for the energetically favored generation/growth of a crack is derived from the energy balance for the generation of the virtual dislocations.

The approach [50] operates with the configurational force F defined as the elastic energy released when the crack moves over a unit distance. In the situation with the plane strain state of an elastically isotropic solid with a dislocation, examined in the paper [44], F can be written in its general form as follows [50]:

$$F = L\,\pi\,(1-\nu)\left(\tilde{\sigma}_{yy}^2 + \tilde{\sigma}_{xy}^2\right)/4G, \qquad (1)$$

where G is the shear modulus, ν is the Poisson ratio, and $\tilde{\sigma}_{yy}$ and $\tilde{\sigma}_{xy}$ are the mean weighted values of the dislocation stress tensor components σ_{yy} and σ_{xy}, respectively. These mean weighted stress tensor components are calculated using the following formula [50]:

$$\tilde{\sigma}_{iy} = 2\,(L\pi)^{-1}\int \sigma_{iy}(x, y=0)[x/L - x)]^{1/2}\mathrm{d}x, \qquad (2)$$

where $i = x, y$.

The equilibrium length L_e of the nanocrack is derived from the balance $F = 2\gamma_e$ between the release F of the elastic energy and the increase $2\gamma_e$ in the energy due to the formation of two new nanocrack surfaces. Each surface is characterized by the energy density γ_e. In the situation where the nanocrack nucleates in the grain interior ((Fig. 4f), we have $\gamma_e = \gamma$, with γ being the energy density per unit area of the free surface. In the situation where the nanocrack nucleates along a grain boundary (Fig. 4g), we have $\gamma_e = \gamma - \gamma_s/2$, with γ_s being the energy density per unit area of the grain boundary. The nucleation of the triple junction nanocrack (Fig. 4f, g) is energetically favorable, if $F > 2\gamma_e$, and unfavorable, if $F < 2\gamma_e$.

In [44], dependences of configurational force F (in units of) $Gb/[16\pi(1\text{-}\nu)]$ on non-dimensional length L/b of the nanocrack were calculated. Here b is the Burgers vector magnitude of a grain boundary dislocation (typical value of b is around 0.1 nm). These dependences are presented in Fig. 5, for the shear stress $\tau = 0.01$G, the Poisson ratio $\nu = 0.3$, the free surface energy density $\gamma = 0.01Gb$, different values of the grain boundary energy density γ_s, different values of the angle α_1 between the nanocrack plane and one of grain boundary planes (see Fig. 4f, g). Also, these dependences are sensitive to values of $n = 5$ and 10, where n is the number of passes of mobile grain boundary dislocations through the triple junction. [In other terms, n characterizes the Burgers vector of the sessile grain boundary (super)dislocation.] The equilibrium length of the nanocrack corresponds to the point where the curve F (L/b) and the horizontal line

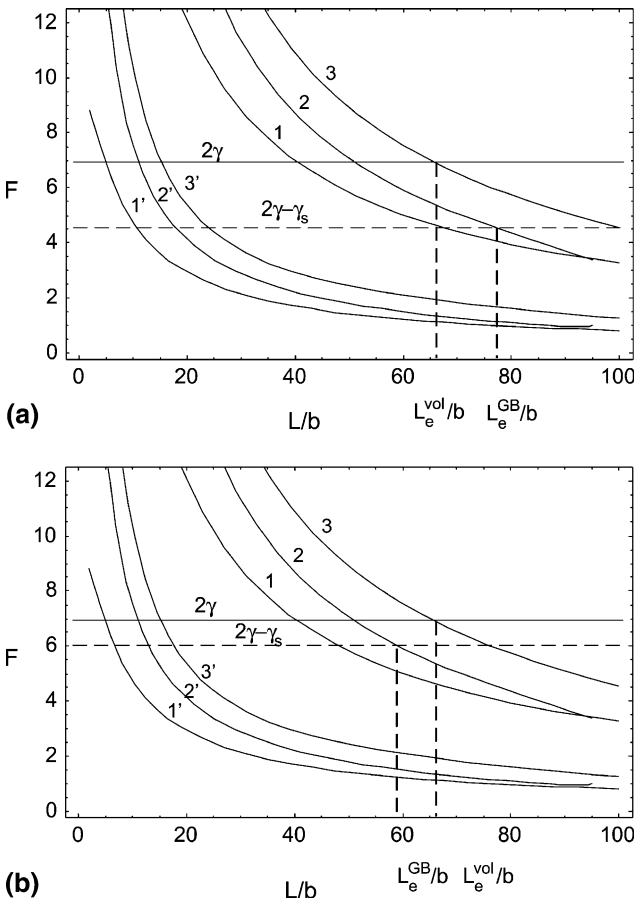

Fig. 5 Dependence of configurational force F (in units of $Gb/[16\pi(1-\nu)]$) on non-dimensional length L/b of the nanocrack, for $r/G = 0.01$, $\nu = 0.3$; $n = 10$ and $\alpha_1 = -\pi/3$, $\pi/3$ and $2\pi/3$ (see *curves 1, 2 and 3*, respectively) as well as $n = 5$ and, $\alpha_1 = -\pi/3$, $\pi/3$ and $2\pi/3$ (see *curves 1′, 2′ and 3′*, respectively). *Horizontal lines* show values of the effective surface energy density $2\gamma_e$ (in units of $Gb/[16\pi(1-\nu)]$) in the cases of the nanocrack nucleating in the grain interior (*solid line*) and along grain boundary plane (*dashed line*), for $\gamma/(Gb) = 0.1$ and $\gamma_s/(Gb) = 0.07$ (**a**) and $\gamma_s/(Gb) = 0.03$ (**b**)

(solid line in the case of the nanocrack nucleating in the grain interior, and dashed line in the case of the nanocrack nucleating along a grain boundary plane) intersect. In Fig. 5, the equilibrium length of the nanocrack in grain interior and along a grain boundary is denoted as L_e^{vol} and L_e^{GB}, respectively.

The notion of a nanocrack (or, more generally, crack) has its sense when the nanocrack length is larger than some critical minimum length L_c at which the binding between the atoms of the opposite surfaces of the nanocrack is completely broken. (L_c is around 5a = 15b, where a is the crystal lattice parameter.) In this context, the generation of a nanocrack is treated to occur, if its equilibrium length $L_e > L_c$. In the opposite case ($L_e < L_c$), the binding between the atoms of the

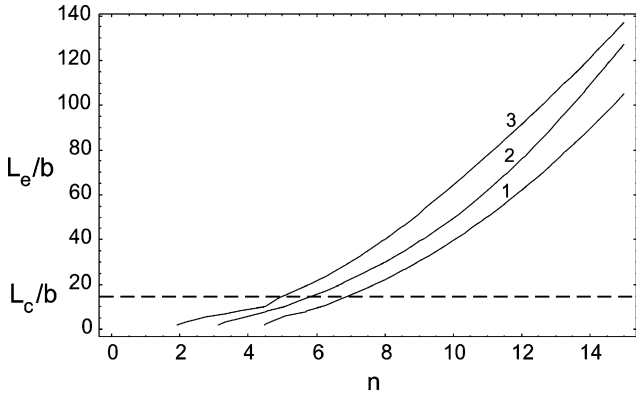

Fig. 6 Dependencies of non-dimensional equilibrium nanocrack length L_e/b on parameter n, for $\beta = 2\pi/3$, $\tau/G = 0.01$, $\nu = 0.3$; $\alpha_1 = -\pi/3$, 0 and $2\pi/3$ (see *curves 1, 2 and 3*, respectively). The *dashed horizontal line* corresponds to the minimum critical length $L_c = 15b$ at which the nanocrack is generated

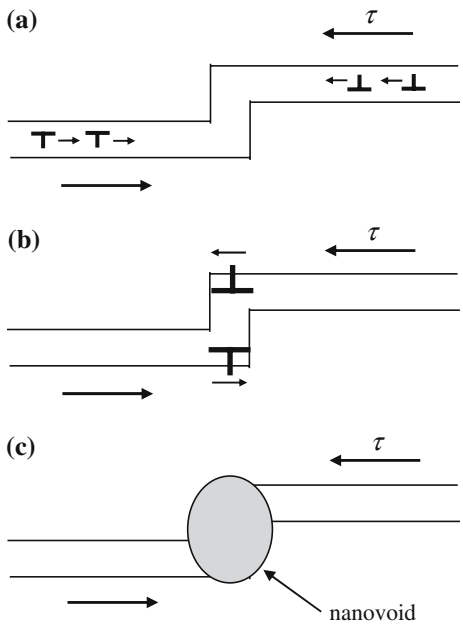

Fig. 7 Grain boundary sliding (**a**) is carried by grain boundary dislocations and (**b**) causes the formation of dipole of dislocations with large Burgers vectors at a grain boundary step. (**c**) Stress fields of dislocations at grain boundary step induce the generation of nanovoid

opposite surfaces of the nanocrack causes it to shrink and disappear.

Ovid'ko and Sheinerman [44] calculated the dependences of the equilibrium length L_e of a nanocrack at a dislocated triple junction on the parameter n, the number of passes of mobile grain boundary dislocations through the triple junction. These dependences are shown in Fig. 6, for the shear stress $\tau = 0.01G$, the Poisson ratio $\nu = 0.3$ and different values of the angle α_1 between the nanocrack plane and one of grain boundary planes. As follows from Fig. 6, the equilibrium length L_e rapidly increases with rising parameter n in both the cases of the nanocrack growing in the grain interior and along a grain boundary. The dashed horizontal line in Fig. 6 corresponds to the critical minimum length $L_c = 15b$ of a nanocrack. The points where this horizontal line intersects the curves L_e (n) correspond to the values of n at which the nanocracks are generated. These values are close to 5, indicating that a stable nanocrack is nucleated at a triple junction after just several (about five) acts of the grain boundary dislocation transformation (Fig. 4) have occurred at the triple junction. Also, L_e grows when the angle β (shown in Fig. 4f, g) between grain boundary planes decreases.

Following calculations [44], the equilibrium length L_e rapidly falls with increasing the free surface energy density γ_e. In general, the equilibrium length L_e^{GB} of a nanocrack nucleating along a grain boundary plane can be either larger or lower than the equilibrium length L_e^{vol} of a nanocrack nucleating in grain interior. The former case ($L_e^{GB} > L_e^{vol}$) is realized at large values of the grain boundary energy density γ_s. In doing so, the nucleation of the triple junction nanocrack growing along a grain boundary is energetically preferred compared to the nanocrack growing in the grain interior. The second case ($L_e^{GB} < L_e^{vol}$) is realized at low values of γ_s. In this case, the nucleation of the triple junction nanocrack growing in the grain interior is preferred.

We have considered the nucleation of nanocracks at triple junctions of grain boundaries in nanocrystalline materials in the situation where grain boundary sliding effectively operates. Recently a theoretical model [53] has been suggested describing the generation of nanovoids at grain boundaries in such nanocrystalline materials. In the framework of the model [53], nanovoids are generated in the stress fields of dipoles of dislocations characterized by large Burgers vectors and formed at both grain boundary steps and junctions due to intensive grain boundary sliding (Fig. 7).

The theoretical models [44, 53] account for experimental observation [23] of nanocracks nucleated at grain boundaries and their triple junctions in deformed nanocrystalline Ni specimens exhibiting a substantial ductility. These specimens were fabricated by elecrodeposition methods, taking care about absence of nanocracks and nanovoids in the as-prepared state. Therefore, nanocracks observed by Kumar et al. [23] in "in situ" experiments during plastic deformation in nanocrystalline Ni are induced by deformation processes. Notice that the models [44, 53] predict a certain

stability of nanocracks generated at grain boundaries and their triple junctions in deformed nanocrystalline materials. This prediction is in agreement with experiments [23] in which a good ductility of nanocrystalline Ni and a non-catastrophic character of failure processes have been detected.

Suppression of nanocrack nucleation in nanocrystalline materials

In this section, we consider mechanisms for suppression of the nanocrack generation in nanocrystalline materials showing ductility or superplasticity. First, let us discuss the effects of diffusion on the generation of triple junction nanocracks treated as typical elemental carriers of fracture in these materials. Generally speaking, diffusivity of nanocrystalline materials is highly accelerated, because of accelerated diffusivity along grain boundaries (compared to the bulk diffusivity) whose amount is large in such materials. Besides, grain boundary diffusion can be highly enhanced in deformed materials due to the action of lattice dislocation slip which 'supplies' dislocations to grain boundaries where these trapped dislocations climb, split into grain boundary dislocations and annihilate. These transformations of dislocations cause the intensive generation of excess grain boundary point defects that carry diffusion in grain boundaries; see, e.g., [54–56]. The accelerated grain boundary diffusion gives rise to the three following effects responsible for suppression of nucleation of triple junction nanocracks: (i) The enhanced diffusion provides both intensive flow of vacancies from the local regions where high tensile stresses of the sessile triple junction dislocations exist and intensive flow of interstitial atoms in the opposite direction (Fig. 8). In these circumstances, the tensile stresses, in part, are relaxed, and the nucleation of nanocracks is hampered [57]. The discussed effect of diffusion gives rise to an increase of the critical plastic strain value at which triple junction nanocracks (Fig. 4f, g) are generated. In certain ranges of parameters of a nanocrystalline solid, diffusion is able of even suppressing the nanocrack generation near triple junctions during the extensive stage of plastic deformation [57]. (ii) Sessile dislocations formed at triple junctions due to grain boundary sliding come into reactions with dislocations that intensively climb along grain boundaries. These dislocation reactions diminish the Burgers vector magnitudes of the sessile dislocations and thereby decrease the stress concentration at triple junctions. Consequently, the grain boundary dislocation climb, whose rate is controlled by grain boundary diffusion, hampers the nanocrack generation at triple junctions of grain boundaries [58]. (iii) The enhanced grain boundary diffusion provides the effective action of Coble creep [59–61] and triple junction diffusional creep [62] which thereby effectively compete with grain boundary sliding. Consequently, the contribution of grain boundary sliding to plastic flow decreases, in which case growth of Burgers vectors of the sessile dislocations—nuclei of triple junction nanocracks (Fig. 4f, g)—slows down or stops.

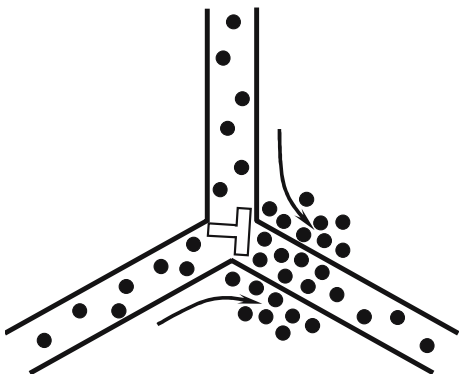

Fig. 8 Diffusional flow of interstitial atoms causes a partial relaxation of tensile stresses created by triple junction dislocation

It is natural to think that the three effects (i)–(iii) of grain boundary diffusion (enhanced owing to the action of conventional lattice dislocation slip) give rise to enhanced ductility exhibited by nanocrystalline materials and materials with bimodal (nano- plus micro-grained) structures, as well as to high-strain-rate superplasticity exhibited by nanocrystalline materials. In doing so, the combined action of lattice dislocation slip and grain boundary sliding as dominant deformation modes is crucial. These deformation modes cause mutually consistent plastic flow of both grain interiors and grain boundaries. In addition, the lattice dislocation slip provides ''bombardment'' of grain boundaries by lattice dislocations which lead to enhancement of boundary diffusion. The enhanced diffusion suppresses nucleation of grain-boundary-sliding-induced nanocracks in nanocrystalline materials which thereby exhibit a good ductility or even superplasticity (for details, see [53]). In particular, the discussed theoretical representations about the diffusion effects on ductility/superplasticity of nanocrystalline materials are indirectly supported by the experimental data [16] showing degradation of superplastic properties of nanocrystalline materials after a short thermal treatment. More precisely, Islamgaliev et al. [16] reported that nanocrystalline materials fabricated by severe plastic deformation method and then subjected to a short heat treatment do not show superplastic behavior,

in contrast to as-fabricated materials. In the experiment [16], heat treatment is not intensive enough to cause grain growth but is sufficient to induce annihilation of the non-equilibrium grain boundary vacancies generated in nanocrystalline materials during their fabrication by severe plastic deformation. In terms of the model [53], after heat treatment, the density of grain boundary vacancies abruptly decreases and thereby the grain boundary diffusion (occurring mostly by vacancy transport) becomes a low-intensity process which is not able to suppress the nanocrack nucleation. As a result, though a nanocrystalline specimen in its as-fabricated state shows superplasticity, heat treatment leads to its dramatic degradation.

Similar effects of diffusion can enhance ductility of materials with bimodal structure; see, e.g., [63]. In general, a material with bimodal structure consists of either ultrafine-grained or nanocrystalline matrix and large (micron-sized) grains embedded into the matrix [21, 27, 63–66]. Such materials are often characterized by both high strength and good ductility [21, 27, 63–66]. Recently, Han et al. [63] have experimentally revealed that a decrease of plastic strain rate in mechanical tests enhances ductility of bimodal 5083 Al alloys processed by cryomilling. Also, they found that the higher ductility at lower strain rate is caused by effective diffusion-mediated stress relaxation, which hamper microcrack nucleation and growth.

When the nucleation of brittle nanocracks is effectively suppressed by diffusion, a material tends to exhibit the ductile fracture behavior. With decreasing temperature, diffusion intensity dramatically decreases. Therefore, one may expect nanocrystalline materials to be brittle at low temperatures. However, following experimental data [67, 68], several nanocrystalline metals (Ni, Co, Cu, Ti, Fe) at liquid-nitrogen temperature (77 K) show a good tensile ductility and a remarkable increase in strength compared to that at room temperature. Enhanced tensile ductility of nanocrystalline materials at cryogenic temperatures is attributed to the effect of temperature on the strain hardening in these materials during plastic deformation. The fact is that the suppression of the nucleation of brittle nanocracks is just one factor necessary for good tensile ductility. Another key factor is the resistance of a material to plastic strain instability leading to the neck formation followed by relatively fast ductile fracture process in the neck section. The resistance is provided by strain hardening and/or pronounced strain rate sensitivity of a material during tensile deformation [27, 67, 68]. Following [27, 67, 68], the strain hardening is enhanced by the dislocation accumulation and depressed by the dislocation annihilation at grain boundaries in deformed nanocrystalline materials. The dislocation annihilation is not intensive at low temperatures, in which case grain boundaries gradually accumulate dislocations providing the moderate strain hardening and thereby the resistance of a material to plastic strain instability [27, 67, 68].

Thus, one can distinguish the two competing effects of temperature on ductility of nanocrystalline materials. With decreasing temperature, both diffusion and dislocation annihilation at grain boundaries are depressed. Low-intensity diffusion is not effective in suppression of the nucleation/growth of brittle cracks. It means that a decrease in temperature causes the suppressing effect on ductility. On the other hand, low-intensity annihilation of dislocations at grain boundaries gives rise to the pronounced strain hardening in nanocrystalline materials deformed at cryogenic temperatures. It means that a decrease in temperature causes the enhancing effect on ductility. In the context discussed, some critical temperature may exist at which the competing effects of temperature are effectively optimized providing a good ductility. Further experimental and theoretical research in this area is needed to reveal critical temperature and other parameters that control and optimize tensile ductility of nanocrystalline materials.

Ductile and brittle fracture modes in nanocrystalline materials: crack growth

Though diffusion effectively suppresses the nanocrack nucleation in several nanocrystalline materials showing superplasticity, the effects of diffusion are not sufficient to suppress fracture in most materials in which nanocracks are intensively generated under mechanical load. Besides, nanocrystalline materials often contain nanocracks formed during their fabrication; see, e.g., [1]. The behavior of nanocracks and plastic flow processes under mechanical load are responsible for the fracture mode operating in a nanocrystalline specimen. At the first stage of loading, flat nanocracks are generated along grain boundaries in the specimen (Fig. 9a, b). If plastic flow is not intensive, these flat nanocracks serve as dangerous stress concentrators inducing new flat nanocracks to be generated in their vicinities (Fig. 9c–e). Then nanocracks located in one specimen section fastly converge resulting in brittle intergranular fracture through the formation of a catastrophic crack (Fig. 9f). If plastic flow and diffusion are intensive, as-generated flat nanocracks (Fig. 10a, b) are gradually transformed into nanovoids (Fig. 10c). Nanovoids grow and are transformed into microvoids

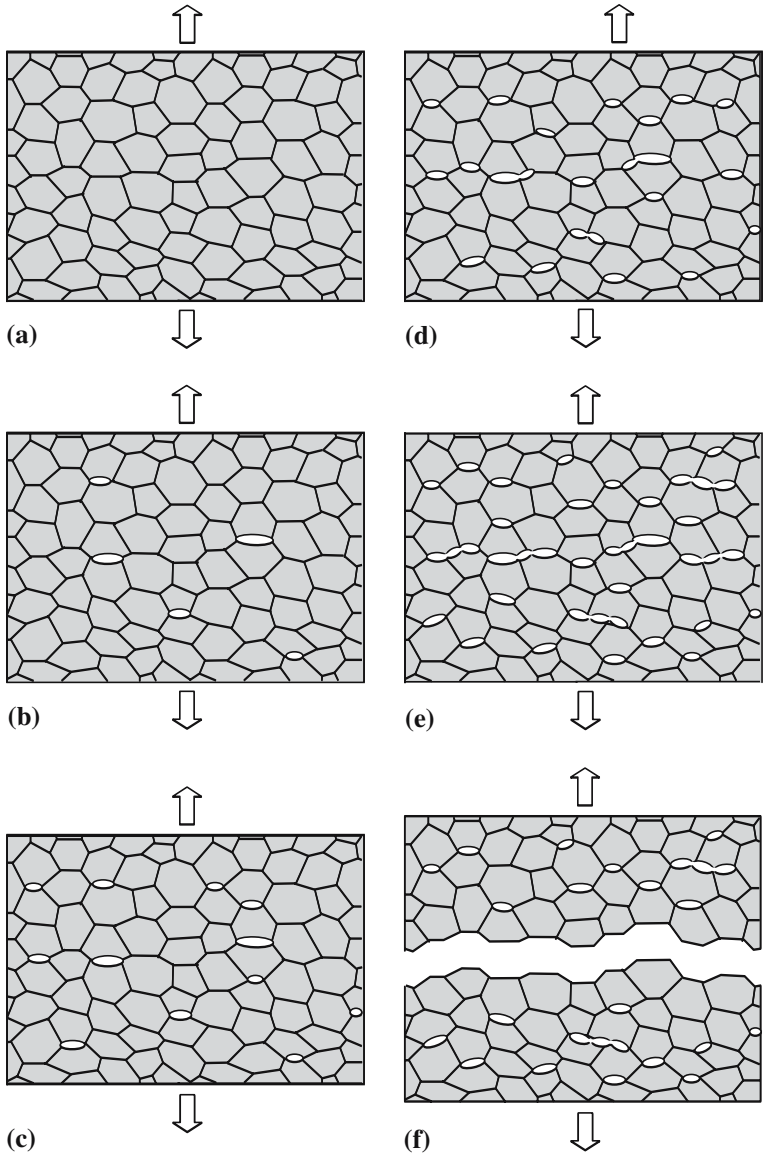

Fig. 9 Intergranular brittle fracture in nanocrystalline material with finest grains occurs through formation and convergence of nanocracks at grain boundaries

(Fig. 10d, e). Plastic flow is localized and gives rise to the neck formation (Fig. 10d, e). Then ductile fracture occurs though coalescence of microvoids located in one specimen section of a nanocrystalline specimen (Fig. 10f).

As noted in section *Ductile and brittle fracture modes in nanocrystalline materials: general aspects*, both intergranular brittle fracture morphology [32, 33, 69] and ductile dimples at fracture surfaces [4, 23, 28–33, 70] were experimentally observed in nanocrystalline materials. A theoretical investigation of nucleation and growth of nanopores—carriers of ductile fracture—in nanocrystalline materials is in its infancy [71]. In contrast, much attention has been paid to computer and theoretical models of brittle fracture processes. Below we will discuss these models focusing on nucleation and growth of brittle nanocracks.

Computer simulations [41, 42] of crack growth in nanocrystalline Ni with grain size ranging from 5 to 12 nm show the intergranular fracture to be dominant. Intergranular nanocracks at grain boundaries and their triple junctions are found to be generated near the tip of a pre-existent crack (a semi-infinite crack artificially formed in a nanocrystalline simulation block in its initial state) due to stress concentration at the tip. The crack grows by joining the nanocracks at grain boundaries and their triple junctions in its front. In the situation where the pre-existent crack ends at a triple junction in a nanocrystalline Ni sample with the grain size $d = 5$ nm, at the first stage of loading, the crack tip remains at the triple junction, and blunting is observed [41]. With increase of the applied mechanical stress, two new nanocracks are formed at a grain boundary located in vicinity of the crack tip. With further

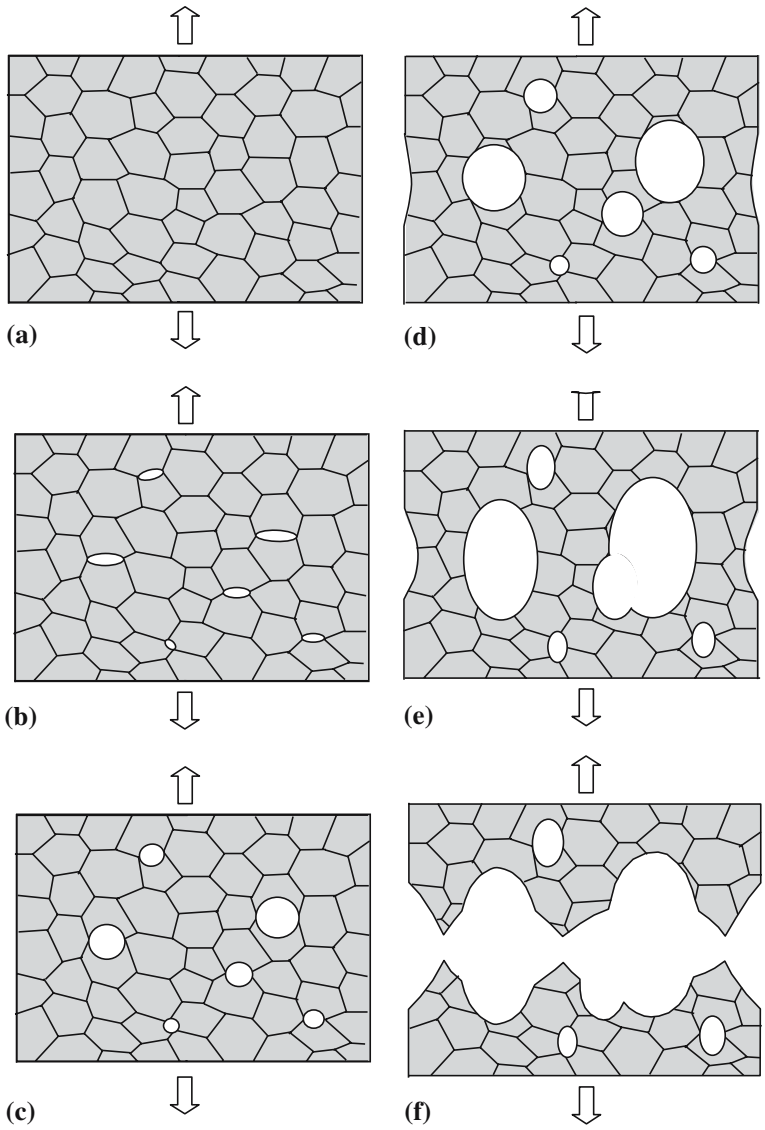

Fig. 10 Ductile fracture in nanocrystalline material occurs through formation of nanocracks, their transformation into pores, growth of pores and formation of local necks between large pores

increase of the applied mechanical stress, the crack grows (by joining the nanocracks) along a path entirely constituted by grain boundaries. In the situation where the pre-existent crack ends in the grain interior in a nanocrystalline Ni sample with the grain size $d = 10$ nm, the crack emits several partial lattice dislocations that blunt the crack tip region. With increase of an applied load, the stress concentration in vicinity of the crack tip causes the formation of nanocracks ahead of the crack front at neighboring grain boundaries. At later stages of loading, these cracks join the main crack [41].

Following computer simulations [41, 42], intergranular fracture processes occurring through growth of a pre-existent crack along grain boundaries is characterized by the energy release rate being approximately three times the expected Griffith value for brittle intergranular fracture. It is indicative of a significant role of plastic flow (realized via emission of partial lattice dislocations and structural transformations in grain boundaries) processes in the intergranular fracture observed in computer simulations [41, 42] of nanocrystalline metals under mechanical load.

Molecular dynamics simulations [41, 42], in fact, dealt with toughness of nanocrystalline Ni. Also, toughness of nanocrystalline materials has been theoretically examined in papers [72, 73] describing brittle crack growth in such materials. Focuses were placed on the competition between intergranular and intragranular fracture modes. In terms of the surface energy density γ_e and grain boundary energy density γ_s, intragranular and intergranular fracture modes (Fig. 10a, b, respectively)

in a coarse-grained polycrystal release the specific energies (per unit area of fracture surface) 2γ and $\gamma_e = \eta(2\gamma - \gamma_s)$, respectively, where η is the factor characterizing fracture surface curvature in the case of intergranular fracture. Nanocrystalline materials with the finest grains are specified by very large volume fractions occupied by grain boundaries and their triple junctions. In these circumstances, ''pure'' intragranular fracture mode cannot be realized. When a flat crack grows in such a material (Fig. 11a), it propagates through regions occupied by grain interiors, grain boundaries and triple junctions. In doing so, a crack releases the energy density:

$$\gamma_{\text{flat}} \approx f_b\gamma_e + f_{gb}\gamma_s + f_{tj}\gamma_{tj}, \tag{3}$$

where f_b, f_{gb} and f_{tj} are the volume fractions occupied by the bulk, grain boundaries and triple junctions, respectively, and γ_{tj} is the specific energy density of triple junctions. In the context discussed, the toughness of a nanocrystalline sample with a flat crack is characterized by parameter [73]:

$$G_c \approx G_b f_b + G_{gb} f_{gb} + G_{tj} f_{tj}, \tag{4}$$

where G_b, G_{gb} and G_{tj} are the critical energy release rates for the bulk, grain boundary and triple junction phases, respectively.

In the case of intergranular brittle fracture, the generation of mode I nanocracks is enhanced along grain boundaries whose planes have a favored orientation, that is, planes at which the action of the external stress is maximum. (A mode I crack is defined as a crack whose generation is accompanied by displacements of its two surfaces in opposite directions normal to the surfaces, parallel to the applied force. Mode I cracks are most conventional in solids.) For any other grain boundary, the external stress action is reduced by a factor (<1) depending on misorientation between the grain boundary plane and the plane having the favored orientation (for details, see [72–74] and a discussion below).

Nanocracks—carriers of brittle intergranular fracture—nucleate and grow along grain boundaries. Grain boundary planes change their orientations at triple junctions whose amount is very large in nanocrystalline materials. In these circumstances, change of nanocrack growth direction at triple junctions represents a critical elemental process of the brittle intergranular fracture, because the crack growth conditions are highly sensitive to crack orientation. To theoretically characterize change of nanocrack growth direction at triple junctions, a theoretical model [75] has been proposed

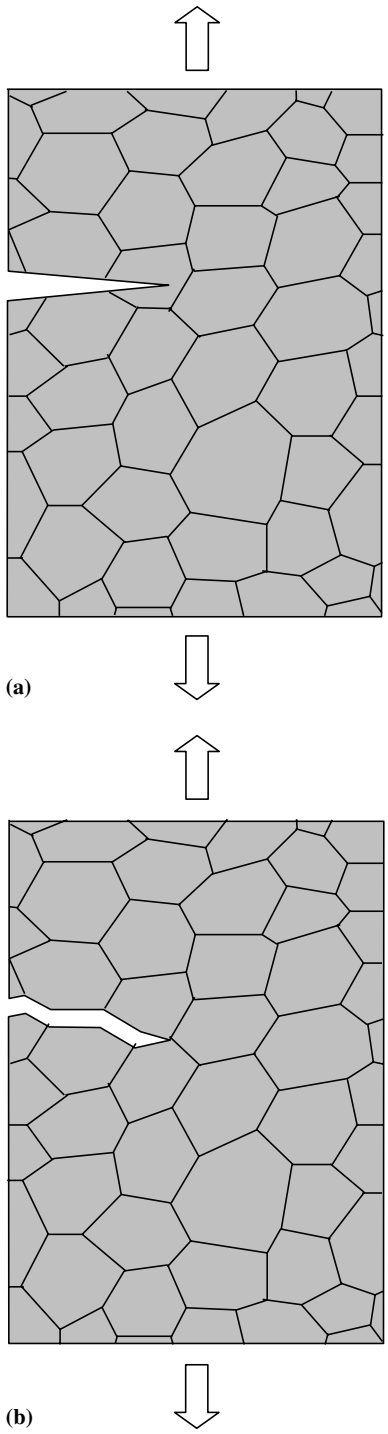

Fig. 11 Crack growth modes in nanocrystalline materials. (**a**) Flat cracks, (**b**) curved cracks growing along grain boundaries

describing the generation and evolution of curved nano-scale cracks (nanocracks) in single-phase nanocrystalline materials and nanocomposites, respectively. In the framework of the model, the nanocracks are nucleated and grow along grain boundaries, changing the direction of their growth at triple junctions.

Intergranular brittle fracture as a percolation process in nanocrystalline materials

We have considered theoretical models and computer simulations of the generation of sole flat and curved nanocracks in the external stress and stress fields of internal stress sources like grain boundary defects and a pre-existent large crack. In general, besides the generation of individual nanocracks, their convergence crucially influences the fracture behavior of brittle nanocrystalline materials. In a paper [74], a theoretical model was suggested focusing on intergranular brittle fracture associated with evolution of nanocrack ensembles in mechanically loaded nanocrystalline materials. In the framework of this model, events of the nanocrack convergence in a nanocrystalline solid are described as elemental events of a percolation process resulting in the formation of catastrophic macroscale crack.

Following the model [74], let us consider a nanocrystalline solid under tensile stress σ_0 (Fig. 9a). At some critical values of the external stress, nanocracks—elemental carriers of intergranular brittle fracture—are formed in the mechanically loaded nanocrystalline solid (Fig. 9b). Following [3], it is assumed that stable nanocracks are formed along grain boundaries and do not penetrate into grain interiors. In doing so, with nanoscopic scales of nanocracks at grain boundaries and large angles made by adjacent grain boundary planes at triple junctions, the formation of a flat nanocrack at a grain boundary is assumed to be independent of the events of the formation of a nanocrack at any other grain boundaries. Consequently, when the external stress increases, new stable flat nanocracks at grain boundaries are formed (Fig. 9c–e). Then the formation of a macroscopic crack—a carrier of the catastrophic failure—occurs (Fig. 9f) which results from elementary independent events of the formation of flat nanocracks at grain boundaries of a quasi-statically loaded nanocrystalline solid.

The macroscopic crack formation under consideration is a partial case of percolation described by the standard mathematical methods of the theory [76–78] of percolation in physical systems. Using these methods, Morozov et al. [74] theoretically described evolution of the nanocrack ensemble in a deformed nanocrystalline solid. In doing so, according to the general representations of the percolation theory [76–78], the macroscopic crack is supposed to be formed when the concentration ρ of stable nanocracks reaches some critical value ρ_c. (In the situation under consideration, the nanocrack concentration ρ is defined as the ratio of the number of grain boundaries at which nanocracks are formed to the total number of grain boundaries.)

A nanocrack of length $2a$ at a grain boundary with length $2a$ and normal n to the grain boundary plane is stable, if $\sigma_{nn} > \sigma_c(d)$. Here σ_{nn} is the stress tensor component at the boundary, and $\sigma_c(a)$ is the critical normal stress characterizing the formation of a stable nanocrack. The critical stress σ_c (a) in the first approximation is given by Griffith's formula [3]:

$$\sigma_c(d) = k(\gamma\ E/d)^{1/2}, \tag{5}$$

where γ denotes the specific surface energy of the solid, E the Young modulus, and k the factor taking into account the nanocrack geometry. Here, for simplicity, one considers the only normal failure mode I, neglecting the shear fracture mode II. [Failure mode I is carried by I mode cracks briefly discussed in the previous section. Failure mode II is carried by II mode cracks each being defined as a crack whose generation is accompanied by relative shear of its two surfaces in the same plane (coinciding with the planes of the surfaces).]

For a grain boundary (and, therefore, a nanocrack formed at this boundary) whose plane has the normal n making the angle α with axis x, we have $\sigma_{nn} = \sigma_0(\cos\alpha)^2$. In this situation, the condition $\sigma_{nn} > \sigma_c(d)$ is sensitive to both grain size and grain boundary orientation characterized by a and α, respectively. With both log-normal distribution in grain size and random distribution in grain boundary orientation in a nanocrystalline specimen, Morozov et al. [74] used the percolation theory methods to calculate the stress $\sigma_{catastrophic}$ at which a catastrophic crack results from independent events of the nucleation of stable nanocracks. The main result of these calculations is that the distributions in grain size and grain boundary orientation, inherent to nanocrystalline solids, do not essentially influence the macroscopic crack formation in the solid. Values of the stress $\sigma_{catastrophic}$ were found to be close to the critical normal stress σ_c (<d>) characterizing the stable state of a nanocrack at a grain boundary with the length equal to the mean grain size <d>. That is, the crucial effect on the macroscopic crack formation is due to the mean grain size which causes the stress $\sigma_{catastrophic}$ at which a catastrophic crack is formed [74]. The percolation theory approach to a theoretical description of fracture processes in nanocrystalline materials is worth being developed in the future to take into account both the interaction between nanocracks and plastic flow effects.

Concluding remarks

Thus, intergranular brittle fracture and ductile fracture are experimentally observed in nanocrystalline materials. Plastic flow in such materials occurs at very high stresses close to those needed to induce fracture. Therefore, nanocracks and nanovoids are easily nucleated in nanocrystalline materials, as with brittle coarse-grained polycrystals [79, 80]. Typical elemental nanocracks in deformed nanocrystalline materials are flat nanocracks nucleated at grain boundaries and their triple junctions due to grain boundary sliding (Fig. 3). Besides such nanocracks, fabrication-produced nanocracks and pores often exist in these materials and decrease their ductility. Evolution of typical nanocracks and nanovoids in a mechanically loaded nanocrystalline specimen causes fracture mode operating in the specimen and depends on its structural characteristics (first of all, grain size), diffusivity and material parameters.

In nanocrystalline materials with finest grains, plastic flow is conducted by mostly grain boundary processes. Deformation mechanisms mediated by curved and short grain boundaries in such materials do not provide effective relaxation of stress buildup at grain boundary steps, triple junctions and elemental flat nanocracks. In these circumstances, new flat nanocracks are easily generated at triple junctions due to grain boundary sliding and stress concentration at neighboring flat nanocracks (Fig. 9). Consequently, intergranular brittle fracture tends to occur in materials with finest grains (Fig. 9).

In nanocrystalline materials with intermediate grains, plastic flow is often conducted by both lattice dislocation slip and grain boundary processes. If plastic flow and diffusion are intensive in these materials, they can provide effective relaxation of stress buildup at triple junctions and elemental flat nanocracks. These flat nanocracks gradually transform into ball-like and elliptic pores (Fig. 10). Due to their shape geometry, stress concentration at ball-like and elliptic nanopores is not so dramatic compared to flat nanocracks. Consequently, such pores slowly grow (by vacancy coagulation at pores and lattice dislocation emission from pores) and cause ductile fracture (Fig. 10). However, if plastic flow and diffusion are not intensive in nanocrystalline materials with intermediate grains and/or these materials contain pre-existent nanocracks and pores, brittle fracture tends to occur.

To summarize, with available results of experimental research, computer simulations and theoretical models of fracture of nanocrystalline materials, one can distinguish the three factors crucially affecting ductility of these materials: the presence of fabrication-induced nanocracks and pores, grain size and diffusivity of grain boundaries. Fabrication-induced nanocracks and pores evidently decrease ductility. Grain size strongly influences fracture mode. Nanocrystalline materials with intermediate grains can show ductile fracture behavior, if plastic flow and diffusion are intensive. Intergranular brittle fracture mode often is dominant in materials with finest grains. High diffusivity (in particular, high diffusivity of non-equilibium grain boundaries) enhances ductility. These three factors and their effects on fracture processes in nanocrystalline materials are of particular interest for future research efforts in this area.

Acknowledgements This work was supported, in part, by the Office of US Naval Research (grant N00014-05-1-0217), INTAS (grant 03-51-3779), INTAS-AIRBUS (grant 04-80-7339), Civilian Research and Development Foundation (grant # RUE2-2684-ST-05), Program of Support of Leading Scientific Schools (grant NSh-4518.2006.1 of the President of Russian Federation) and Russian Academy of Sciences Program 'Structural Mechanics of Materials and Construction Elements'.

References

1. Koch CC, Morris DG, Lu K, Inoue A (1999) MRS Bull 24:54
2. Gleiter H (2000) Acta Mater 48:1
3. Veprek S, Argon AS (2002) J Vac Sci Technol 20:650
4. Kumar KS, Suresh S, Van Swygenhoven H (2003) Acta Mater 51:5743
5. Milligan WW (2003) Mechanical behavior of bulk nanocrystalline and ultrafine-grain metals. In: Milne I, Ritchie RO, Karihaloo B (eds) Comprehensive structural integrity. Elsevier, Amsterdam, p 529
6. Valiev RZ (2004) Nature Mater 3:511
7. Gutkin MY, Ovid'ko IA (2004) Plastic deformation in nanocrystalline materials. Springer, Berlin Heidelberg New York
8. Ovid'ko IA (2005) Int Mater Rev 50:65
9. Ovid'ko IA (2005) Rev Adv Mater Sci 10:89
10. Han BQ, Lavernia E, Mohamed FA (2004) Rev Adv Mater Sci 9:1
11. Wolf D, Yamakov V, Phillpot SR, Mukherjee AK, Gleiter H (2005) Acta Mater 53:1
12. Lu C, Mai YW, Shen YG (2006) J Mater Sci 41:937
13. Mayo MJ (1997) Nanostruct Mater 9:717
14. Mishra RS, Valiev RZ, Mcfadden SX, Mukherjee AK (1998) Mater Sci Eng A 252:174
15. Mcfadden SX, Mishra RS, Valiev RZ, Zhilyaev AP, Mukherjee AK (1999) Nature 398:684
16. Islamgaliev RK, Valiev RZ, Mishra RS, Mukherjee AK (2001) Mater Sci Eng A 304–306:206
17. Valiev RZ, Song C, Mcfadden SX, Mukherjee AK, Mishra RS (2001) Phil Mag A 81:25
18. Mishra RS, Valiev RZ, Mcfadden SX, Islamgaliev RK, Mukherjee AK (2001) Phil Mag A 81:37
19. Valiev RZ, Alexandrov IV, Zhu YT, Lowe TC (2002) J Mater Res 17:5
20. Mukherjee AK (2002) Mater Sci Eng A 322:1

21. Wang Y, Chen M, Zhou F, Ma E (2002) Nature 419:912
22. Champion Y, Langlois C, Guerin-Mailly S, Langlois P, Bonnentien J-L, Hytch M (2003) Science 300:310
23. Kumar KS, Suresh S, Chisholm MF, Norton JA, Wang P (2003) Acta Mater 51:387
24. Zhan G-D, Kuntz JD, Wan J, Mukherjee AK (2003) Nanomaterials for structural applications. Berndt CC, Fisher T, Ovid'ko IA, Skandan G, Tsakalakos T (eds) MRS Symp. Proc., vol 740, Warrendale, p 49
25. He G, Eckert J, Loeser W, Schultz L (2003) Nature Mater 2:33
26. He G, Hagiwara M, Eckert J, Loeser W (2004) Phil Mag Lett 84:365
27. Wang YM, Ma E (2004) Acta Mater 52:1699
28. Youssef KM, Scattergood RO, Murty KL, Koch CC (2004) Appl Phys Lett 85:929
29. Youssef KM, Scattergood RO, Murty KL, Horton JA, Koch CC (2005) Appl Phys Lett 87:091904
30. Cheng S, Ma E, Wang YM, Kecskes LJ, Youssef KM, Koch CC, Trociewitz UP, Han K (2005) Acta Mater 53:1521
31. Youssef KM, Scattergood RO, Murty KL, Koch CC (2006) Scr Mater 54:251
32. Li H, Ebrahimi F (2004) Appl Phys Lett 84:4307
33. Li H, Ebrahimi F (2005) Adv Mater 17:1969
34. Moser B, Hanlon T, Kumar KS, suresh S (2006) Scr Mater 54:1151
35. Liao XZ, Zhou F, Lavernia EJ, Srinivasan SG, Baskes MI, He DW, Zhu YT (2003) Appl Phys Lett 83:632
36. Liao XZ, Zhou F, Lavernia EJ, He DW, Zhu YT (2003) Appl Phys Lett 83:5062
37. Liao XZ, Srinivasan SG, Zhao YH, Baskes MI, Zhu YT, Zhou F, Lavernia EJ, Hu HF (2004) Appl Phys Lett 84:3564
38. Wu X-L, Zhu YT, Ma E (2006) Appl Phys Lett 88:121905
39. Lubarda VA, Schneider MS, Kalantar DH, Remington BA, Meyers MA (2004) Acta Mater 52:1397
40. Hugo RC, Kung H, Weertman JR, Mitra R, Knapp JA, Follstaedt DM (2003) Acta Mater 51:1937
41. Farkas D, Van Swygenhoven H, Derlet PM (2002) Phys Rev B 66:060101
42. Van Swygenhoven H, Derlet PM, Hasnaoui A, Samaras M (2003) In: Tsakalakos T, Ovid'ko IA, Vasudevan AK (eds) Nanostructures: synthesis, functional properties and applications. Kluwer, Dordrecht, p 155
43. Latapie A, Farkas D (2004) Phys Rev B 69:134110
44. Ovid'ko IA, Sheinerman AG (2004) Acta Mater 52:1201
45. Conrad H, Narayan J (2000) Scr Mater 42:1025
46. Sutton AP, Balluffi RW (1996) Grain boundaries in crystalline materials. Oxford Sci., Oxford
47. Bobylev SV, Ovid'ko IA (2006) Phys Rev B 73:064102
48. Fedorov AA, Gutkin MY, Ovid'ko IA (2003) Acta Mater 51:887
49. Gutkin MY, Ovid'ko IA, Skiba NV (2004) Acta Mater 52:1711
50. Indenbom VI (1961) Sov Phys Sol State 3:1506
51. Gutkin MY, Ovid'ko IA (1994) Phil Mag A 70:561
52. Rybin VV, Zhukovskii IM (1978) Sov Phys Sol State 20:1056
53. Ovid'ko IA, Sheinerman AG (2006) Phil Mag 86:3487
54. Ovid'ko IA, Reizis AB (2001) Phys Sol State 43:35
55. Ovid'ko IA, Sheinerman AG (2003) Phil Mag 83:1551
56. Perevezentsev VN, Pupynin AS, Svirina JV (2005) Mater Sci Eng A 410–411:273
57. Ovid'ko IA, Sheinerman AG (2005) Acta Mater 53:1347
58. Ovid'ko IA, Sheinerman AG (2004) Rev Adv Mater Sci 6:21
59. Masumura RA, Hazzledine PM, Pande CS (1998) Acta Mater 46:4527
60. Kim HS, Estrin Y, Bush MB (2000) Acta Mater 48:493
61. Yamakov V, Wolf D, Phillpot SR, Gleiter H (2002) Acta Mater 50:61
62. Fedorov AA, Gutkin MY, Ovid'ko IA (2002) Scr Mater 47:51
63. Han BQ, Huang JY, Zhu YT, Lavernia EJ (2006) Acta Mater 54:3015
64. Tellkamp VL, Melmed A, Lavernia EJ (2001) Met Mater Trans. A 32:2335
65. Zhang X, Wang H, Koch CC (2004) Rev Adv Mater Sci 6:53
66. Sergueeva AV, Mara NA, Mukherjee AK (2004) Rev Adv Mater Sci 7:67
67. Wang YM, Ma E (2004) Appl Phys Lett 85:2750
68. Wang YM, Ma E, Valiev RZ, Zhu Y (2004) Adv Mater 16:328
69. Gan Y, Zhou B (2001) Scr Mater 45:625
70. Mukai T, Suresh S, Kita K, Sasaki H, Kobayashi N, Higashi K, Inoue A (2003) Acta Mater 51:4197
71. Ovid'ko IA, Sheinerman AG (2006) Phil Mag 86:1415
72. Pozdnyakov VA (2003) Tech Phys Lett 29:151
73. Pozdnyakov VA, Glezer AM (2005) Phys Sol State 47:817
74. Morozov NF, Ovid'ko IA, Petrov YV, Sheinerman AG (2003) Rev Adv Mater Sci 4:65
75. Gutkin MY, Ovid'ko IA (2004) Phil Mag Lett 84:655
76. Ziman J (1949) Models of disorder. Cambridge University Press, Cambridge
77. Stauffer D, Aharony A (1992) Introduction to percolation theory. Taylor and Francis, London
78. Sahimi M (1994) Applications of percolation theory. Taylor and Francis, London
79. Ashby MF, Gandhi C, Taplin DMR (1979) Acta Mater 27:699
80. Gandhi C, Ashby MF (1979) Acta Mater 27:1565